A novel control approach for the fixed-time synchronization of the complex network

Xu Xu, Zongying Li, Tuiruo Yan and Eric Li

***Abstract*—A novel fixed-time controller is proposed for the complex networks using the hyperbolic sine function instead of the sum of the two power functions that are usually used in the existing fixed-time approaches. Compared with some existing results, the proposed controller is simpler with only a few parameters, and can ensure the higher convergence and tighter bound for the settling time. In addition, the proposed controller does not include the sign function of the error and avoids the chattering effects. The sufficient conditions are established to guarantee that the synchronization error converges exactly to zero in a fixed-time interval. Three numerical experiments have clearly verified the theoretical results.** [1]

***Index Terms*—Complex networks; synchronization; fixed-time; chattering effects, settling time**

I. INTRODUCTION

Over the past decades, synchronization in complex networks (CNs) has drawn widespread attention due to its potential applications in secure communication, image process, biological systems, information science, et al. [1-3]. For the synchronization of CNs, the Lyapunov direct method is usually used to give the asymptotic or exponential behavior, where the system's trajectories converge to zero in an infinite amount of time. However, the infinite convergence time is impossible in practical applications. In order to enhance convergence, the fixed-time control has been proposed recently, and can drive the system convergence within a settling time without depending on the original conditions [4-6]. In Ref. [7-8], the following fixed-time controller was proposed

$$\mathrm{u}(t) = -\kappa \mathrm{e}(t) - \eta_1 \operatorname{sgn}(\mathrm{e}) |\mathrm{e}|^{\varepsilon} - \eta_2 \operatorname{sgn}(\mathrm{e}) |\mathrm{e}|^{\xi}, \tag{1}$$

where $\kappa,\ \eta_1,\ \eta_2 > 0$, $0 < \varepsilon < 1,\ \xi > 1$, e is the system error. As Eq. (1) includes the sign function of the error, it can cause the chattering phenomena. In [9-**Error! Reference source not found.**], the continuous controller (2) was proposed

$$\mathrm{u}(t) = -\kappa \mathrm{e}(t) - \eta_1 \mathrm{e}^{\varepsilon/\mu} - \eta_2 \mathrm{e}^{\xi/\rho},\ i \in \mathrm{Z}_+ = \{1,2,...,N\} \tag{2}$$

where $\varepsilon, \mu, \xi, \rho$ are all odds satisfying $\varepsilon < \mu$ and $\xi > \rho$. Due to not having the sign function, the jumping and chattering phenomena are avoided. In Ref. [13], a simpler controller

$$\mathrm{u}(t) = -\eta_1 \mathrm{e}^{\varepsilon/\mu} - \eta_2 \mathrm{e}^{\xi/\rho}. \tag{3}$$

was proposed. Compared with the controllers (1) and (2), Eq. (3) does not include the linear control term, and thus needs more time to achieve convergence. In addition, the settling time is larger than that from the controllers (1) and (2).

Up to now, the most fixed-time controllers had the power terms like $\eta_1 \operatorname{sgn}(\mathrm{e})|\mathrm{e}|^{\varepsilon} + \eta_2 \operatorname{sgn}(\mathrm{e})|\mathrm{e}|^{\xi}$ or $\eta_1 \mathrm{e}^{\varepsilon} + \eta_2 \mathrm{e}^{\xi}$ with $0 < \varepsilon < 1$ and $\xi > 1$, where the controllers include 4 parameters η_1, η_2 ε and ξ. Thus, a question is raised: can one design a simpler continuous fixed-time controller with fewer parameters? To date, few studies have focused on such work. This paper proposes a novel fixed-time controller. Compared with some existing results, the controller has the following advantages: (1) it uses the hyperbolic sine function instead of the power functions (2) it is simpler only including two parameters; (3) it ensures the higher convergence and tighter bound for the settling time; (4) it does not include the sign function and avoid the chattering effects.

II. MODEL AND PRELIMINARIES

This paper considers the following CN with N nodes

$$\dot{\mathrm{x}}(t) = \mathrm{g}(\mathrm{x}(t)) + (\mathrm{A} \otimes \Gamma)\,\mathrm{x}(t) + \mathrm{u}(\mathrm{x}(t)), \tag{4}$$

where $\mathrm{x} = \mathrm{col}(\mathrm{x}_1, \mathrm{x}_2, ..., \mathrm{x}_N) \in \mathrm{R}^{nN}$ is the state vector with $\mathrm{x}_i \in \mathrm{R}^n$ for $i \in \mathrm{Z}_+$, $\mathrm{g}(\mathrm{x}) = \mathrm{col}(g(\mathrm{x}_1), g(\mathrm{x}_2), ..., g(\mathrm{x}_N))$ with $g(\mathrm{x}_i) \in \mathrm{R}^n$ governs the intrinsic dynamics of the node, $\Gamma \in \mathrm{R}^{n\times n}$ is the inner coupling matrix, $\mathrm{A} = \{a_{ij}\}_{N\times N}$ is the connection weight matrix satisfying $a_{ii} = -\sum_{j=1, j\neq i}^{N} a_{ij}$, where $a_{ij} \neq 0$ if there is a link from node j to i ($i \neq j$); $a_{ij} = 0$ otherwise, $\mathrm{u}(\cdot)$ is the control input. The aim of this paper is to ensure the synchronization of all nodes in network with the manifold $\mathrm{x}_1 = \mathrm{x}_2 = ... = \mathrm{x}_N = s(t)$, where $s(t) \in \mathrm{R}^n$ is defined as

$$\dot{s}(t) = g(s(t)), \tag{5}$$

with initial value $s(0) = s_0$.

Definition 1: The CN (4) is said to be globally synchronized with (5) within a fixed time, if there exists a settling time $T^* > 0$, which is independent of the initial values $\mathrm{x}_i(0)$ and $\mathrm{s}(0)$ such that $\lim_{t\to T_*} \|\mathrm{x}_i(t) - \mathrm{s}(t)\| = 0$ and $\|\mathrm{x}_i(t) - \mathrm{s}(t)\| = 0$ for $t \geq T_*$, for all $i \in \mathrm{Z}_+$.

Notation: For any vector $\mathrm{y} = (y_1, y_2, \cdots, y_m)^{\mathrm{T}} \in \mathrm{R}^m$, define

Manuscript received xxx xx 2021. This work was supported in part by the National Natural Scientific Foundation of China (NSFC) (12072128), and the Special Funds of Provincial Industrial Innovation of Jilin Province China (No. 2017C028-1), and Project of Science and Technology Development of Jilin Province China (No. 20190201302JC) .

X. Xu, Z. Li, and T. Yan are with the College of Mathematics, Jilin University, Jilin 130012, China (e-mail: 1909268378@qq.com and xuxu@jlu.edu.cn). (*Corresponding author: Xu Xu.*)

E. Li is with the School of Computing, Engineering & Digital Technologies, Teesside University, Middleborough, United Kingdom (e-mail: ericsg2012@gmail.com).

(a): $\mathrm{y}^{\theta}=(y_1^{\theta}, y_2^{\theta}, \cdots, y_m^{\theta})^{\mathrm{T}}$, θ is a positive odd.

(b): $|\mathrm{y}|=(|y_1|,|y_2|,\cdots,|y_m|)^{\mathrm{T}}$, $|\cdot|$ denotes absolute value.

Assumption 1: There exists a constant $\rho>0$ such that:

$$(\mathrm{y}\text{-}\mathrm{z})^{\mathrm{T}}[\mathrm{g}(\mathrm{y})\text{-}\mathrm{g}(\mathrm{z})] \le \rho(\mathrm{y}\text{-}\mathrm{z})^{\mathrm{T}}(\mathrm{y}\text{-}\mathrm{z}),\ \forall \mathrm{y}, \mathrm{z} \in \mathrm{R}^{nN}.$$

Lemma 1 [14]: For the symmetric matrix $\mathrm{A}\in\mathrm{R}^{m\times m}$, one has

$$\mathrm{y}^{\mathrm{T}}\mathrm{A}\,\mathrm{y} \le \lambda_{\max}(\mathrm{A})\,\mathrm{y}^{\mathrm{T}}\mathrm{y},\ \forall\, \mathrm{y}\in\mathrm{R}^{m},$$

where $\lambda_{\max}(\mathrm{A})$ denotes the maximum eigenvalue of A.

Lemma 3 [14]: If $a_i\ge 0$, $i=1,2,\cdots,n$ and $0<r\le 1$, $s>1$ then: $\sum_{i=1}^n a_i^r \ge (\sum_{i=1}^n a_i)^r$, and $\sum_{i=1}^n a_i^s \ge n^{1-s}(\sum_{i=1}^n a_i)^s$.

Lemma 4 [7]: If there is a non-negative function $V(t)$ satisfying $\dot V(t)\le -\alpha V^p-\beta V-\gamma V^q$, then we have $V(t)\equiv 0$ when $t>T^1$, where $T^1=\frac{1}{\beta(1-p)}\ln(1+\frac{\beta}{\alpha})+\frac{1}{\beta(q-1)}\ln(1+\frac{\beta}{\gamma})$,with $\alpha>0$, $\beta>0$, $\gamma>0$, $0<p<1$, $q>1$.

III. Fixed-time Synchronization

Denote $\mathrm{e}(t)=\mathrm{col}(\mathrm{e}_1,\mathrm{e}_2,...,\mathrm{e}_N)$ with $\mathrm{e}_i(t)=\mathrm{x}_i(t)-s(t)$, $i\in\mathrm{Z}_+$. Then from (4) and (5) one has:

$$\dot{\mathrm{e}}(t)=\mathrm{g}(\mathrm{x})-\mathrm{g}(\mathrm{s})+(\mathrm{A}\otimes\mathrm{P})\mathrm{e}+\mathrm{u}(\mathrm{x},\mathrm{s}), \qquad (6)$$

From Definition 1, the fixed-time synchronization (FTS) of the coupled nodes of Eq. (4) to the trajectory (5) is equivalent to the globally fixed-time stability of the trivial equilibrium of the error system (6).

In this work, the following controller is constructed:

$$\mathrm{u}(t)=-\kappa\mathrm{e}(t)-\mathrm{sh}(\eta\mathrm{e}^{\varepsilon}), \qquad (7)$$

where $\kappa>0$, $\varepsilon=\varepsilon_1/\varepsilon_2$ where both ε_1 and ε_2 are positive odd integers satisfying $\varepsilon_1<\varepsilon_2$, $\mathrm{sh}(\cdot)$ denotes the hyperbolic sine function: $\mathrm{sh}(y)=(\exp(y)+\exp(-y))/2$ for $\forall y\in\mathrm{R}$.

Remark 1: In Eq. (7), function $\mathrm{sh}(\eta\mathrm{e}^{\varepsilon})$ is used to construct the fixed-time controller instead of the power function similar to $\alpha\mathrm{e}^p+\beta\mathrm{e}^q$ [9]. Besides κ, control (7) only has two parameters η and ε. Compared with the existing results [9, 10], controller (7) is simpler and is easier to implement in practical problems.

Remark 2: Compared with existing results [7], control (7) is continuous and differential without the sign function of the error, and avoids the chattering phenomena.

Theorem 1: If Assumption 1 holds, the CN (4) is globally synchronized with (5) by control (7), if $\kappa>\rho+\lambda_{\max}(\mathrm{A}\otimes\Gamma)$; and the settling time is

$$T_*=\frac{1}{\beta(1-p)}\ln(1+\frac{\beta}{\alpha})+\frac{1}{\beta(q-1)}\ln(1+\frac{\beta}{\gamma+(\sum_{k>J}\gamma_k)}),$$

where the parameters are defined in (8), (10) and (13).

Proof: Consider the energy function $V(t)=\mathrm{e}^{\mathrm{T}}(t)\mathrm{e}(t)/2$. Using Assumption 1, Lemma 1 and control (7), the time derivation of $V(t)$ along the error trajectory (6) is

$$\begin{aligned}\dot V(t)&=\mathrm{e}^{\mathrm{T}}[\mathrm{g}(\mathrm{x})-\mathrm{g}(\mathrm{s})+(\mathrm{A}\otimes\Gamma)\mathrm{e}+\mathrm{u}]\\&\le[\rho+\lambda_{\max}(\mathrm{A}\otimes\Gamma)-\kappa]\mathrm{e}^{\mathrm{T}}\mathrm{e}-\mathrm{e}^{\mathrm{T}}\mathrm{sh}(\eta\mathrm{e}^{\varepsilon})\\&=-\beta V-\mathrm{e}^{\mathrm{T}}\mathrm{sh}(\eta\mathrm{e}^{\varepsilon}),\end{aligned} \qquad (8)$$

where $\beta\equiv 2[\kappa-\rho-\lambda_{\max}(\mathrm{A}\otimes\Gamma)]>0$. Using Taylor expansion $\mathrm{sh}(x)=\sum_{k=1}^{+\infty}\frac{1}{(2k-1)!}(x)^{2k-1}\ \forall x\in\mathrm{R}$, we have:

$$\begin{aligned}\mathrm{e}^{\mathrm{T}}\mathrm{sh}(\eta\mathrm{e}^{\varepsilon})&=\textstyle\sum_{i=1}^N\sum_{j=1}^n e_{ij}\mathrm{sh}(\eta e_{ij}^{\varepsilon})\\&=\textstyle\sum_{i=1}^N\sum_{j=1}^n[e_{ij}\sum_{k=1}^{+\infty}\frac{1}{(2k-1)!}(\eta e_{ij}^{\varepsilon})^{2k-1}].\end{aligned} \qquad (9)$$

From Taylor expansion of $\mathrm{sh}(\cdot)$, for a given ε, there exists a positive integer J such that $(2J-1)\varepsilon>1$, and $(2J-3)\varepsilon\le 1$. Denote $\sigma=(2J-1)\varepsilon$, then (9) can be written as

$$\begin{aligned}&\mathrm{e}^{\mathrm{T}}\mathrm{sh}(\eta\mathrm{e}^{\varepsilon})\\&\ge\textstyle\sum_{i=1}^N\sum_{j=1}^n e_{ij}[\eta e_{ij}^{\varepsilon}+\frac{\eta^{2J-1}}{(2J-1)!}(e_{ij}^{\varepsilon})^{2J-1}+\sum_{k>J}\frac{\eta^{2k-1}}{(2k-1)!}(e_{ij}^{\varepsilon})^{2k-1}]\\&=\textstyle\sum_{i=1}^N\sum_{j=1}^n[\eta(e_{ij}^2)^{\frac{1+\varepsilon}{2}}+\mu(e_{ij}^2)^{\frac{1+\sigma}{2}}+\sum_{k>J}\mu_k(e_{ij}^2)^{\frac{1+\sigma_k}{2}}]\\&=\textstyle\sum_{i=1}^N\sum_{j=1}^n[\eta(e_{ij}^2)^p+\mu(e_{ij}^2)^q+\sum_{k>J}\mu_k(e_{ij}^2)^{q_k}]\end{aligned} \qquad (10)$$

where $p=\frac{1+\varepsilon}{2}$, $q=\frac{1+\sigma}{2}$, $\mu=\frac{\eta^{2J-1}}{(2J-1)!}$, $\sigma_k=(2k-1)\varepsilon$, $\mu_k=\frac{\eta^{2k-1}}{(2k-1)!}$, $q_k=\frac{1+\sigma_k}{2}$ with $k>J$. It is easy to see $\sigma_k>\sigma>1$, and thus $q_k>q>1$. Using Lemma 3, Eq. (10) gives

$$\begin{aligned}\mathrm{e}^{\mathrm{T}}\mathrm{sh}(\eta\mathrm{e}^{\varepsilon})&\ge\eta[\textstyle\sum_{i=1}^N\sum_{j=1}^n(e_{ij}^2)]^p+\mu(nN)^{\frac{1-\sigma}{2}}[\sum_{i=1}^N\sum_{j=1}^n(e_{ij}^2)]^q\\&\quad+\textstyle\sum_{k>J}\{\mu_k(nN)^{1-q_k}[\sum_{i=1}^N\sum_{j=1}^n(e_{ij}^2)]^{q_k}\}\\&=\eta(2V)^p+\mu(nN)^{1-q}(2V)^q\\&\quad+\textstyle\sum_{k>J}[\mu_k(nN)^{1-q_k}(2V)^{q_k}]\end{aligned} \qquad (11)$$

Substituting (11) into (8) yields

$$\dot V(t)\le-\beta V-\alpha V^p-\gamma V^q-\textstyle\sum_{k>J}(\gamma_k V^{q_k})=-r(V), \qquad (12)$$

where $p=(1+\varepsilon)/2$, and thus $p\in(1/2,\ 1)\subset(0,1)$, and

$$\alpha=2^p\eta,\ \gamma=2^q\mu(nN)^{1-q},\ \gamma_k=2^{q_k}\mu_k(nN)^{1-q_k}. \qquad (13)$$

To consider the fixed time synchronization, we consider the following integral:

$$\begin{aligned}T&\le\int_0^{\sup V(x)}\frac{1}{r(V)}\mathrm{d}V<\int_0^1\frac{\mathrm{d}V}{r(V)}+\int_1^{+\infty}\frac{\mathrm{d}V}{r(V)}\\&\le\int_0^1\frac{\mathrm{d}V}{\beta V+\alpha V^p}+\int_1^{+\infty}\frac{\mathrm{d}V}{\beta V+\gamma V^q+\sum_{k>J}(\gamma_k V^{q_k})}\end{aligned} \qquad (14)$$

It is noted that $q_k>q$. Therefore, when $V>1$, we have

$$\begin{aligned}&\textstyle\sum_{k>J}(\gamma_k V^{q_k})=\sum_{k>J}(\gamma_k V^q V^{q_k-q})\\&>\min_{k>J}(V^{q_k-q})\textstyle\sum_{k>J}(\gamma_k V^q)>\sum_{k>J}(\gamma_k V^q)\end{aligned} \qquad (15)$$

Substituting (15) into (14), we have

$$T\le\int_0^1\frac{\mathrm{d}V}{\beta V+\alpha V^p}+\int_1^{+\infty}\frac{\mathrm{d}V}{\beta V+(\gamma+\sum_{k>J}\gamma_k)V^q}. \qquad (16)$$

Using Lemma 4, we have

$$T^*=\frac{1}{\beta(1-p)}\ln(1+\frac{\beta}{\alpha})+\frac{1}{\beta(q-1)}\ln(1+\frac{\beta}{\gamma+\sum_{k>J}(\gamma_k)})<+\infty. \qquad (17)$$

Therefore, according to theorem 5 in Ref. [5], the system is fixed time synchronization and the bound of the settling time shows in Eq. (17) . This completes the proof. ##

Remark 3: The purpose of the hyperbolic function converting into the power function is to give a simple proof of the convergence. In addition, it can give an analytical expression of the bound (17) of the setting time that is tighter compared with that in the existing results.

Remark 4: It is clear that $\gamma_k > 0$ for all $k > J$. So for the same parameters α, β, γ as in Lemma 4, Eq. (17) gives the smaller bound of the settling time, that is $T_* < T^1$.

Remark 5: There are not any special requirements for the adjacent matrix A. So the proposed controller can be used to the directed complex networks.

IV. NUMERICAL SIMULATION

Example 1: FTS in a small world network

Consider a small world network with four nodes. The parameters and the topology are shown in Fig. 1.

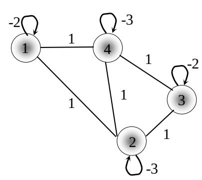

Fig. 1. Schematic diagram of a small world network

All nodes of the network are the Lorenz oscillator describing by $\dot{\mathbf{V}} = [a(y-x), -y + x(d-z), -cz + xy]^{\mathrm{T}}$, where, $a = 10$, $c = 2.67$, $d = 28$ and $\mathbf{V} = (x, y, z)^{\mathrm{T}}$. With these parameters, the Lorenz oscillator exhibits the chaotic motion.

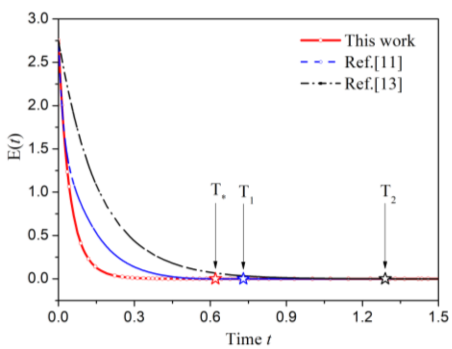

Fig. 2. Comparisons of the error and settling times: the blue, black and red circular lines are the results from the methods in [11], [13] and this work.

The error $E(t) = \sum_{i=1}^{N} \sum_{k=1}^{n} e_{ik}^2(t)$ is used to consider the synchronization. In control (7), we set $\Gamma = I_3$, $\varepsilon = 3/5$, and $\kappa = 3.2$, $\eta = 2$ to satisfy the conditions of Theorem 1. Fig. 2 gives the simulations depicting the time history of $E(t)$ for the same initial conditions. It is clear that the $E(t)$ arrives at zero ($< 1.0e-5$) in about 0.18 seconds, 0.44 seconds, and 0.82 seconds when the proposed methods, Yang's work [11], and Xu's work [13] are used, respectively. In addition, the settling time T^* (0.62s) obtained in our study is much smaller than T_1 (0.73) in Ref. [11] and T_2 (1.29) in Ref. [13]. These results clearly indicate that the proposed method has higher convergence and the tighter bound of the settling time compared with the existing methods.

Fig. 3 illustrates the time history of three components of each node in the network. Each component of node arrives at the same states within the fixed-time. It indicates that the synchronized chaotic motions can also be achieved using the proposed method.

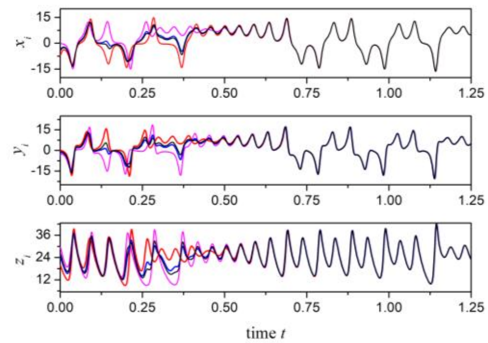

Fig. 3. Chaotic manifold in the $x, y, z-$components.

Fig. 4 shows the evolution of synchronous manifolds. We illustrate the 3-D phase diagrams of the nodes 1 and 2 with the different initial conditions. It is clear that the nodes can track the complex chaotic states.

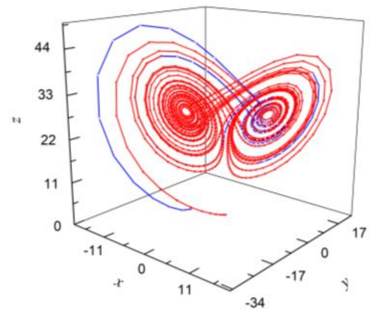

Fig. 4. 3-D phase diagrams of synchronous manifolds

Example 2: FTS in a neural network circuit

We design a circuit with a directed ring artificial neural network shown in Fig. 5. The motion equations are

$$\begin{cases} C\dot{x}_1 = (V_3 - x_1)/R - x_1/r + u_1(t) \\ C\dot{x}_2 = (V_1 - x_2)/R - x_2/r + u_2(t) \\ C\dot{x}_3 = (V_2 - x_3)/R - x_3/r + u_3(t) \end{cases} \tag{18}$$

where x_i denotes the input voltage of the i-th amplifier, $V_i = \tanh(x_i)$ is the output voltage, $C = 10\mathrm{nF}$, $R = 1\mathrm{K}\Omega$, $r = 100\mathrm{K}\Omega$; u_i is control input (7) with $\kappa = 2.4$ and $\eta = 1.2$. In a similar way of the analysis with example 1, Fig. 6 shows the control errors $e_i (i = 1,2,3)$ and the settling time. It is clear that the ring directed neural network can achieve the fixed-time synchronization.

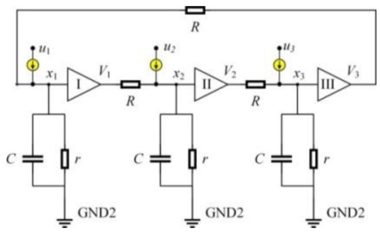

Fig. 5. Circuit diagram of a directed ring neural network

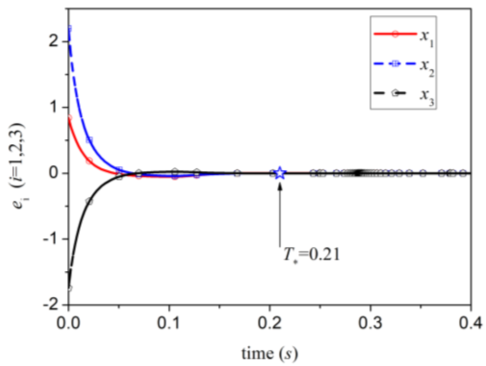

Fig. 6. Synchronization of a directed neural network circuit

Example 3: FTS in a scale free circuit

We study the FTS in a large-scale network with two hundred nodes. The BA scale free network model [15] is used to generate the topology of the networks. Each node is set as a 3-D cellular neural system, which is described by:

$$\dot{\mathbf{y}}_i(t) = -D\mathbf{y}_i + Ag(\mathbf{y}_i) + c\sum_{j=1}^{n} b_{ij}\Gamma\mathbf{y}_j(t) \quad , \qquad (19)$$

where $i \in Z_+$, $\mathbf{y}_i = (y_{i1}, y_{i2}, y_{i3})^{\mathrm{T}}$, $D = \Gamma = \mathbf{I}_3$, $g(\cdot)$ is the activation function, where $g(u) = 0.5(|u+1| - |u-1|)$, and

$$A = \begin{bmatrix} 1.25 & -3 & -4 \\ -3 & 1.1 & -4.5 \\ -4 & 4.5 & 1 \end{bmatrix}.$$

For any $\mathrm{y,z} \in \mathrm{R}^3$, one has

$$\begin{aligned} & g(\mathrm{z}) - g(\mathrm{y}) = -D(\mathrm{y\text{-}z}) + A[g(\mathrm{y}) - g(\mathrm{z})] \\ & \le -(y_1\text{-}z_1, y_2\text{-}z_2, y_3\text{-}z_3)^{\mathrm{T}} + A(|y_1\text{-}z_1|, |y_2\text{-}z_2|, |y_3\text{-}z_3|)^{\mathrm{T}} \\ & \le (\mathrm{I}_3 + A)(|y_1\text{-}z_1|, |y_2\text{-}z_2|, |y_3\text{-}z_3|)^{\mathrm{T}} \end{aligned}$$

Since $\lambda_{\max}(\mathrm{I}_3 + A) = 3.99$, if one sets $\rho = 4.2$, then Assumption 1 holds true for any $\mathrm{y,\ z} \in \mathrm{R}^3$. Since the network models are randomly generated according to predetermined parameters, the convergence is characterized by the average error for 10 runs for each set of parameters. We make a comparison between the proposed method and the existing methods in Ref. [11] and [13], where these methods have the same control parameters and topology in each run with $\varepsilon = 5/7$, $\eta = 2$, $\kappa_i = 11.2$ ($i = 1,2,\ldots,10$) and c=0.5. Figure 7 shows the synchronization error of the system. It is seen that, the synchronization error quickly tends to zero when the controller is imposed, which verifies the convergence of the controlled system. We also compare the average bounds of the settling time in the 10 runs between the proposed method and the existing methods in Ref. [11], and Ref. [13], which shows that the proposed method has the higher convergence.

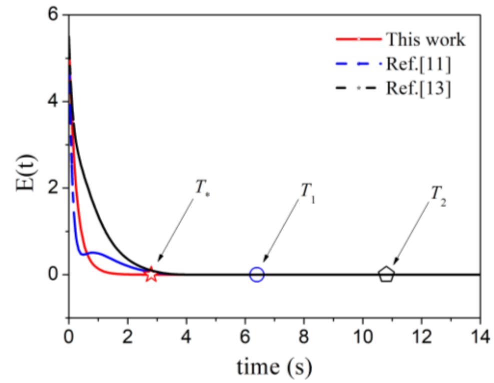

Fig. 8. Comparisons of the error and settling times: the blue, black and red circular lines are the results from the methods in [11], [13] and this work.

From these three examples, it is clearly seen that there are no chattering phenomena by using the proposed controller.

V. Conclusions and Discussions

This work investigates the fixed-time synchronization of the complex networks via a non-chattering controller. First, a function $\mathrm{sh}(\eta\, \mathrm{e}^{\varepsilon})$ is introduced to construct a simpler continuous controller. Compared with most existing works, it has fewer parameters, higher convergence and the tighter bound of the settling time. In addition, the controller does not include the sign function of the error, and guarantees the elimination of the chattering effects. In the proposed approach, we exert control over all nodes to get the fixed-time synchronization. In the real problems, it is impossible or unnecessary to exert control over all nodes. The pinning strategy thus becomes a widely used method by adding the control inputs to a fraction of nodes of the network. On the other hand, the real-world problems usually focus on the non-smooth systems or the system with unknown dynamics, unknown parameters, or the external disturbance [16-20]. So the future work is devoted to designing the pinning strategy, or considering the systems with non-smooth, unknown parameters or disturbances.

Acknowledgment

This work was supported in part by the National Natural Scientific Foundation of China (NSFC) under grant number 12072128, and the Special Funds of Provincial Industrial Innovation of Jilin Province China (No. 2017C028-1), and Project of Science and Technology Development of Jilin Province China (No. 20190201302JC).

References

1 J. Zhou, H. Zhang, L. Xiang, L. and Q. Wu, “Synchronization of coupled harmonic oscillators with local instan-

taneous interaction", *Automatica*, vol. 48, pp. 1715-1721, 2012

2 D. Ibanez-Soria, J. Garcia-Ojalvo, A. Soria-Frisch, and G. Ruffini, "Detection of generalized synchronization using echo state networks", *Chaos*, vol. 28, no. 3, pp. 033118, 2018.

3 X. Xu, D. Y. Yu, and Z. H. Wang, "Inter-layer synchronization of periodic solutions in two coupled rings with time delay", *Physica D*, vol. 396, pp, 1-11, 2019.

4 A. Polyakov, "Nonlinear feedback design for fixed-time stabilization of Linear Control Systems", *IEEE T. Automat. Contr.*, vol. 57, no. 8, pp. 2106-2110, 2012.

5 F. Lopez-Ramirez, D. Efimov1, A. Polyakov1 and W. Perruquetti, "Conditions for fixed-time stability and stabilization of continuous autonomous systems", *Syst. Control Lett.*, vol. 129, pp. 26–35, 2019.

6 A. Polyakov, D. Efimov, and W. Perruquetti, "Finite-time and fixed-time stabilization: Implicit Lyapunov function approach", *Automatica*, vol. 51, pp. 332-340, 2015.

7 C. Chen, L. Li, H. Peng, Y. Yang, L. Mi, and H. Zhao, "A new fixed-time stability theorem and its application to the fixed-time synchronization of neural networks", *Neural Network*, vol. 123, pp. 412-4, 2020.

8 X. Y. Liu, D. W. C. Ho, Q. Song, and J. D. Cao, "Finite-/fixed-time robust stabilization of switched discontinuous systems with disturbances," *Nonlinear Dynam.*, vol. 90, no. 3, pp. 2057–2068, 2017.

9 X. S. Yang, L. James, D. W. C. Ho, and Z. G. Feng, "Fixed-time synchronization of complex networks with impulsive effects via nonchattering control," *IEEE T. Automat. Contr.*, vol. 62, no. 11, pp. 5511–5521, Nov. 2017.

10 W. Zhang, X. Yang, and C. Li, "Fixed-Time Stochastic Synchronization of Complex Networks via Continuous Control", *IEEE T. Cybernetics*, vol. 49, no. 8, pp. 3099-3104, 2019.

11 X. Yang , J. Lam , D. W. C. Ho, Z. Feng, "Fixed-time synchronization of complex networks with impulsive effects via nonchattering Control", *IEEE T. Automat. Contr.*, vol. 62, no. 11, pp. 511-5521, 2017.

12 Y. Liu, M. Liu, X. Xu, "Fixed-time synchronization of stochastic complex networks with Markov jump and mixed delays via adaptive non-chattering control" Optim. Contr. App. Met., https://doi.org/10.1002/oca.2804, 2021.

13 Y. Xu, X.Wu, N. Li, L. Liu, C. Xie and C. Li, "Fixed-time synchronization of complex Networks with a simpler nonchattering controller", IEEE T. Circuits-II. vol. 67, no. 4, pp. 700-704, 2020.

14 T. Kövari, *Inequalities*, Cambridge University Press, USA, 1988.

15 A. L. Barabási, R. Albert, "Emergence of scaling in random networks", Science, vol. 286, pp. 509–512, 1999.

16 Z. Peng, J. Hu, K. Shi, R. Luo, R. Huang, B. K.r Ghosh, J. Huang, "A novel optimal bipartite consensus control scheme for unknown multi-agent systems via model-free reinforcement learning", Appl. Math. Comput. vol. 369, pp. 124821, 2020.

17 L. Hua, H. Zhu, K. Shi, S. Zhong , Y. Tang, Y. Liu, "Novel Finite-Time Reliable Control Design for Memristor-Based Inertial Neural Networks With Mixed Time-Varying Delays", IEEE T. Circuits-I, vol.68, no. 4, pp. 1599-1609, 2021.

18 K. Shia,J. Wang, Y. Tang, S. Zhong, "Reliable asynchronous sampled-data filtering of T–S fuzzy uncertain delayed neural networks with stochastic switched topologies", Fuzzy Set. Syst. Vol. 381, pp. 1–25, 2020.

19 C. Deng, C. Wen, J. Huang, X. Zhang, Y. Zou, "Distributed observer-based cooperative control approach for uncertain nonlinear mASs under event-triggered communication", DOI 10.1109/TAC.2021.3090739

20 C. Deng, F. Guo, C. Wen, D. Yue, Y. Wang, "Distributed resilient secondary control for DC microgrids against heterogeneous communication delays and DoS attacks", DOI 10.1109/TIE.2021.3120492.